Bioorganic & Medicinal Chemistry 18 (2010) 8044–8053

Contents lists available at ScienceDirect

Bioorganic & Medicinal Chemistry

journal homepage: www.elsevier.com/locate/bmc

Anti-leishmanial and anti-trypanosomal activities of 1,4-dihydropyridines: In vitro evaluation and structure–activity relationship study

Juliana Q. Reimão [a], Marcus T. Scotti [b], André G. Tempone [a,*]

[a] Laboratory of Applied Toxinology on Antiparasitic Drugs, Department of Parasitology, Instituto Adolfo Lutz. Avenida Dr. Arnaldo, 351, 8° andar. Cerqueira Cesar, CEP 01246-902 São Paulo, SP, Brazil
[b] Center of Applied Sciences and Education, Federal University of Paraíba, Campus IV, Rio Tinto, PB, Brazil

ARTICLE INFO

Article history:
Received 13 July 2010
Revised 2 September 2010
Accepted 7 September 2010
Available online 15 September 2010

Keywords:
Leishmania
Trypanosoma cruzi
1,4-Dihydropyridines
QSAR

ABSTRACT

Leishmaniasis and Chagas' disease constitute a relevant health and socio-economic problem in Latin America, Africa, and Asia. The therapeutic interventions rely on inefficient and highly toxic drugs with systemic side effects in patients. Considering the multiple biological activities of the calcium channel blockers and the high versatility of 1,4-dihydropyridines, eight clinically used 1,4-dihydropyridines (azelnidipine, amlodipine, cilnidipine, lercanidipine, nicardipine, nifedipine, nimodipine and nitrendipine) were in vitro tested against *Leishmania* and *Trypanosoma cruzi* parasites, and their cytotoxicity was tested against mammalian cells. In addition, a QSAR study was performed in order to delineate further structural requirements for the anti-protozoan activity and to predict the biological potency of 1,4-dihydropyridines. The tested compounds were effective against *Leishmania (L.) amazonensis*, *Leishmania (V.) braziliensis*, *Leishmania (L.) chagasi*, and *Leishmania (L.) major* promastigotes, *L. (L.) chagasi* intracellular amastigotes and *T. cruzi* trypomastigotes with 50% inhibitory concentration (IC_{50}) values in the range of 2.6–181 μM. The QSAR provided useful information about the structural features of the anti-protozoan activities, including diphenylpropyl and diphenylmethylazetidin groups at position 4 of the 1,4-dihydropyridine ring, allowing the prediction of two novel potential anti-protozoan analogs.

1. Introduction

American Trypanosomiasis (Chagas' disease) and Leishmaniasis (Kala-azar) are widespread protozoan diseases that affect mostly poor and marginal populations in Latin America, Africa, and Asia. Neglected by big pharmaceutical companies, the chemotherapy of both diseases involves highly toxic drugs, and in the case of Chagas' disease, an inefficient therapy. Therefore, there is still an urgent need for novel drug candidates in the interest of public health.

Calcium channel blockers are a class of drugs with a selective inhibition of calcium influx through cell membranes, releasing and binding calcium in intracellular pools. These have been widely used in the therapy of hypertension, cerebrovascular spasms, and other pathogeneses.[1] Calcium channel blockers have been considered promising anti-parasitic candidates, and can partially reverse multidrug resistance, presumably by increasing cellular drug accumulation.[2,3] This effect was observed with drug-resistant strains of *Plasmodium falciparum*,[4] *Leishmania donovani*, and *Trypanosoma cruzi*.[5,6] Additionally, the 1,4-dihydropyridines amlodipine and lacidipine have been shown to successfully inhibit *L. donovani* in vitro infection and in BALB/c mice.[7] Furthermore, nimodipine was in vitro effective against promastigotes and intracellular amastigotes of *Leishmania (L.) chagasi*, resulting in strong ultrastructural damage to the mitochondria and plasma membrane.[8]

The physicochemical properties and biological activity of organic compounds depend on their molecular structures. With the purpose of obtaining relationships between chemical structures and biological activities by using computational approaches, it is necessary to find appropriate representations of the molecular structure of the compounds.[9] The encoded information of a molecular descriptor depends on the kind of molecular representation that is used and the defined algorithm for its calculation. Simple molecular descriptors derived from the counting of atom types or structural fragments in the molecule, and others derived from algorithms applied to a topological representations (molecular graphs), are usually called topological or 2D-descriptors. Others molecular descriptors derived from a geometrical representation are called geometrical or 3D-descriptors.[9] Graph-theoretical methods have been very useful in quantitative structure–activity relationship (QSAR) studies in order to perform rational analysis of biological activities.[10] This method allows structural information to be codified and expressed in numbers. Thus, graph-based molecular descriptors have proven to be very efficient in drug design.[11] Many works using graph-theoretical approaches have

* Corresponding author. Tel.: +55 11 3068 2991.
E-mail address: atempone@ial.sp.gov.br (A.G. Tempone).

0968-0896/$ - see front matter © 2010 Elsevier Ltd. All rights reserved.
doi:10.1016/j.bmc.2010.09.015

been reported for the design of new drugs, to control toxicity parameters and to find common structural patterns of known drugs. The successful design of drugs like analgesics,[12] anti-virals,[13] anti-bacterials,[14] and anti-mycobacterials[15] have been reported using this method.

In the present study, eight clinically used 1,4-dihydropyridines were in vitro tested against *Leishmania* and *T. cruzi* parasites, and their cytotoxicity was tested against mammalian cells. In addition, a QSAR study was performed in order to delineate further structural requirements for the anti-protozoan activity and to predict the biological activity of 1,4-dihydropyridines.

2. Results and discussion

2.1. Anti-parasitic activity and mammalian cytotoxicity

The serial dilution of the 1,4-dihydropyridines (Fig. 1 compounds **1**–**8**) and standard drugs allowed determination of the IC_{50} values after cellular viability detection using the oxidative mitochondrial system, as shown in Table 1. The 1,4-dihydropyridines were active against the promastigotes and amastigotes of *L. (L.) chagasi*, the Visceral Leishmaniasis agent in Latin America. Based on the sigmoidal dose–response curves, we obtained IC_{50} values in the range of 2.61–146.41 μM after 24 h of incubation with *L. (L.) chagasi* promastigotes. The activity of the tested compounds against intracellular amastigotes of *L. (L.) chagasi* resulted in IC_{50} values close to promastigotes, in the range of 5.35–176.24 μM, confirming the anti-leishmanial activity of these compounds. Pentavalent antimony was used as a reference drug and gave an IC_{50} value of 82.32 μM against intracellular amastigotes. In addition, this is the first description of amlodipine activity against *Leishmania (L.) amazonensis*, *Leishmania (V.) braziliensis*, *L. (L.) chagasi* and *Leishmania (L.) major*. In a previous work, amlodipine demonstrated in vitro and in vivo activity against *L. (L.) donovani*, the Indian agent of kala-azar, with a promising oral effect at 10 mg/kg in a hamster model.[7] Despite the use of amlodipine in the treatment of hypertension and angina, the in vitro inhibition of cancer cells[16,17] and a strong antimicrobial activity[18] have also been reported, showing the versatility of this compound.

In our model, it was not possible to evaluate the IC_{50} value of azelnidipine on intracellular amastigotes due to the low selectivity (the IC_{50} against amastigotes is very close to the IC_{50} against mammalian cells). The tested compounds were also effective against *L. (L.) amazonensis* and *L. (V.) braziliensis*, the most important Cutaneous Leishmaniasis agents in Brazil, with IC_{50} values in the range of 2.93–128.16 μM against promastigotes. Likewise, the tested compounds were effective against *L. (L.) major*, an agent of Cutaneous Leishmaniasis in the Old World, with IC_{50} values in the range of 3.35–181.09 μM. Pentamidine was used as a standard drug in the promastigotes assay and gave IC_{50} values in the range of 0.15–1.11 μM.

In order to study the effectiveness of calcium channel blockers against *T. cruzi*, trypomastigote forms were incubated with the test compounds for 24 h, resulting in promising IC_{50} values, as shown

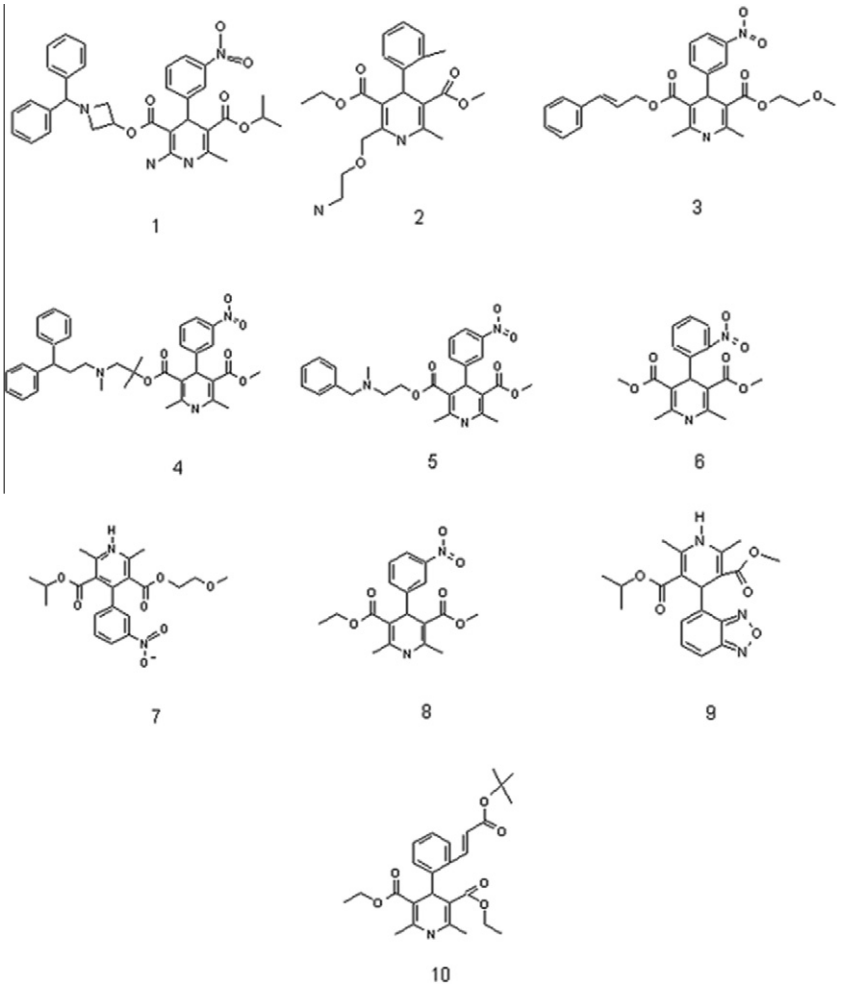

Figure 1. 1,4-Dihydropyridine chemical structures. Compound **1**: azelnidipine; **2**: amlodipine; **3**: cilnidipine; **4**: lercanidipine; **5**: nicardipine; **6**: nifendipine; **7**: nimodipine; **8**: nitrendipine; **9**: isradipine; **10**: lacidipine.

Table 1
Effect of 1,4-dihydropyridines on parasites and mammalian cytotoxicity

Drug	IC_{50} (μM)						
	L. (L.) chagasi promastigotes	*L. (L.) chagasi* amastigotes	*L. (L.) amazonensis* promastigotes	*L. (L.) major* promastigotes	*L. (V.) braziliensis* promastigotes	*T. cruzi* trypomastigotes	LLC-MK2 cytotoxicity
Azelnidipine	33.39 ± 7.91	nd	20.54 ± 5.76	17.06 ± 2.28	13.67 ± 1.15	2.90 ± 0.13	33.48 ± 0.15
Amlodipine	2.61 ± 0.22	5.35 ± 1.03	2.93 ± 0.39	3.35 ± 1.17	3.13 ± 0.3	8.07 ± 0.66	70.82 ± 30.62
Cilnidipine	33.01 ± 7.13	28.42 ± 1.99	110.67 ± 19.47	21.44 ± 1.34	15.26 ± 0.49	5.62 ± 1.28	221.51 ± 34.54
Lercanidipine	19.17 ± 2.42	10.36 ± 0.25	16.95 ± 2.44	11.55 ± 1.12	10.33 ± 1.12	8.43 ± 3.05	434.99 ± 29.67
Nicardipine	35.66 ± 1.06	22.00 ± 1.04	26.50 ± 2.73	21.83 ± 2.39	19.08 ± 3.2	10.59 ± 0.44	71.59 ± 10.44
Nifedipine	146.41 ± 28.04	176.24 ± 6.68	117.89 ± 11.16	181.09 ± 53.78	95.74 ± 10.59	101.75 ± 17.7	588.73 ± 255.64
Nimodipine	82.68* ± 30.43	21.62* ± 7.97	128.16* ± 56.89	31.04* ± 7.18	42.80 ± 1.05	32.31 ± 4.92	96.19* ± 0.32
Nitrendipine	64.13 ± 17.71	43.84 ± 0.92	38.32 ± 6.66	33.27 ± 2.94	39.04 ± 5.76	26.88 ± 3.57	137.72 ± 10.75
Pentamidine	1.11 ± 1.03	nd	0.49 ± 0.05	0.47 ± 0.11	0.15 ± 0.17	nd	25.61 ± 3.99
Glucantime	nd	82.32 ± 3.22	nd	nd	nd	nd	>1366
Benznidazole	nd	nd	nd	nd	nd	172.37 ± 99.13	>1366

IC_{50}: inhibitory concentration 50%; ±: standard error; nd: not determined.
* Data from Tempone et al.[8]

in Table 1. The IC_{50} values ranged from 2.9 to 101.75 μM, suggesting that *T. cruzi* parasites are more susceptible to calcium channel blockers than *Leishmania* parasites. In a previous work, the activity of the 1,4-dihydropyridines lacidipine (IC_{50} value of 33.5 μM) and isradipine (IC_{50} value of 20.8 μM) were demonstrated against *T. cruzi* epimastigotes, resulting in inhibition of the respiratory chain.[19] All tested compounds were considerably more effective against *T. cruzi* than the standard drug benznidazole, which showed an IC_{50} value of 172.37 μM. Our assays demonstrated that 1,4-dihydropyridines presented significant activity against *T. cruzi* trypomastigotes, suggesting the potential activity of these calcium antagonists as anti-parasitic candidates.

Table 2
Selectivity Index (SI) of 1,4-dihydropyridines, given by the ratio between the cytotoxicity toward LLC-MK2 cells and the anti-parasitic activity

Drug	SI	
	L. (L.) chagasi amastigotes	*T. cruzi* trypomastigotes
Azelnidipine	nd	11.54
Amlodipine	13.24	8.77
Cilnidipine	7.79	39.41
Lercanidipine	41.99	51.6
Nicardipine	3.25	6.76
Nifedipine	4.21	5.78
Nimodipine	4.45*	2.98
Nitrendipine	3.14	5.12

nd: not determined.
* Data from Tempone et al.[8]

In order to study the selectivity of 1,4-dihydropyridines against the tested parasites, an in vitro cytotoxicity assay using mammalian cells was carried out for 48 h. It showed IC_{50} values in the range of 33.48–588.73 μM against *Rhesus* monkey kidney cells (LLC-MK2). Pentamidine presented an IC_{50} value of 25.61 μM and was considerably more toxic than the tested 1,4-dihydropyridines. Selectivity is a relevant characteristic for defining lead molecules.[20] Therefore, the Selectivity Index (SI) was used to compare the toxicity for LLC-MK2 cells and the activity against the parasites (Table 2). The 1,4-dihydropyridines demonstrated SI values ranging from 3.12 to 41.99 for *L. (L.) chagasi* amastigotes and from 2.98 to 39.41 for *T. cruzi* trypomastigotes. For both parasites, the highest SI was found for lercanidipine, which is a promising lead molecule for future drug design studies. As a complementary cytotoxicity parameter, the hemolytic activity was also determined using mice erythrocytes, and the 1,4-dihydropyridines showed a lack of hemolytic activity at the highest concentration of 50 μM.

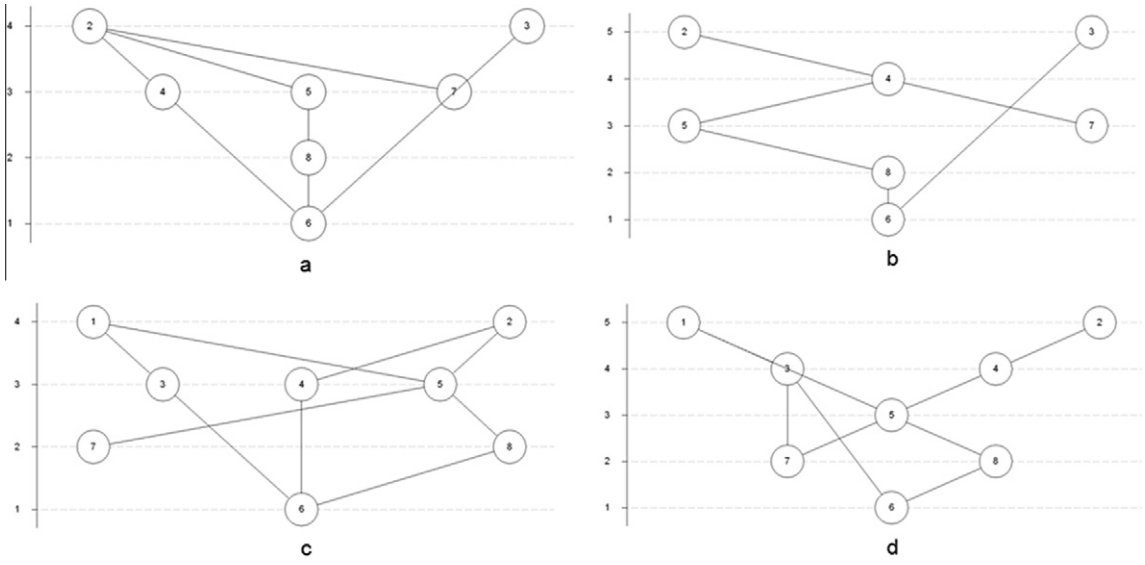

Figure 2. Hasse diagrams: (a) for mammalian cytotoxicity and anti-parasitic activities excluding the compound azelnidipine (**1**); (b) for only anti-parasitic activities excluding the compound azelnidipine (**1**); (c) for mammalian cytotoxicity and anti-parasitic activities excluding the activity against *L. (L.) chagasi* amastigotes; (d) for only anti-parasitic activities excluding the activity against *L. (L.) chagasi* amastigotes.

Nimodipine is clinically used to treat ischemic damage caused by cerebral arterial spasm in subarachnoid hemorrhage.[21] In previous work, nimodipine showed a selective effectiveness against promastigotes, intracellular amastigotes of *L. (L.) chagasi* and promastigotes of *L. (L.) amazonensis* and *L. (L.) major*.[8] In the present work, nimodipine demonstrated a promising anti-parasitic effect against *T. cruzi* and *L. (V.) braziliensis*, confirming the in vitro potential of this compound.

2.2. Analysis of 1,4-dihydropyridine activities (QSAR)

The Hasse diagrams and PCA analyses made it possible to separate the compounds into sets. The first Hasse diagram (Fig. 2a—for all activities, without compound **1**) showed that **2** and **3** were the most active compounds; **4**, 5, and **7** were on the second level, and **8** and **6** were the least active compounds. Therefore, the chain was **2** ⩾ **5** ⩾ **8** ⩾ **6**, **2** ⩾ **4** ⩾ **6**, **2** ⩾ **7**, and finally, **3** ⩾ **6**. Compounds

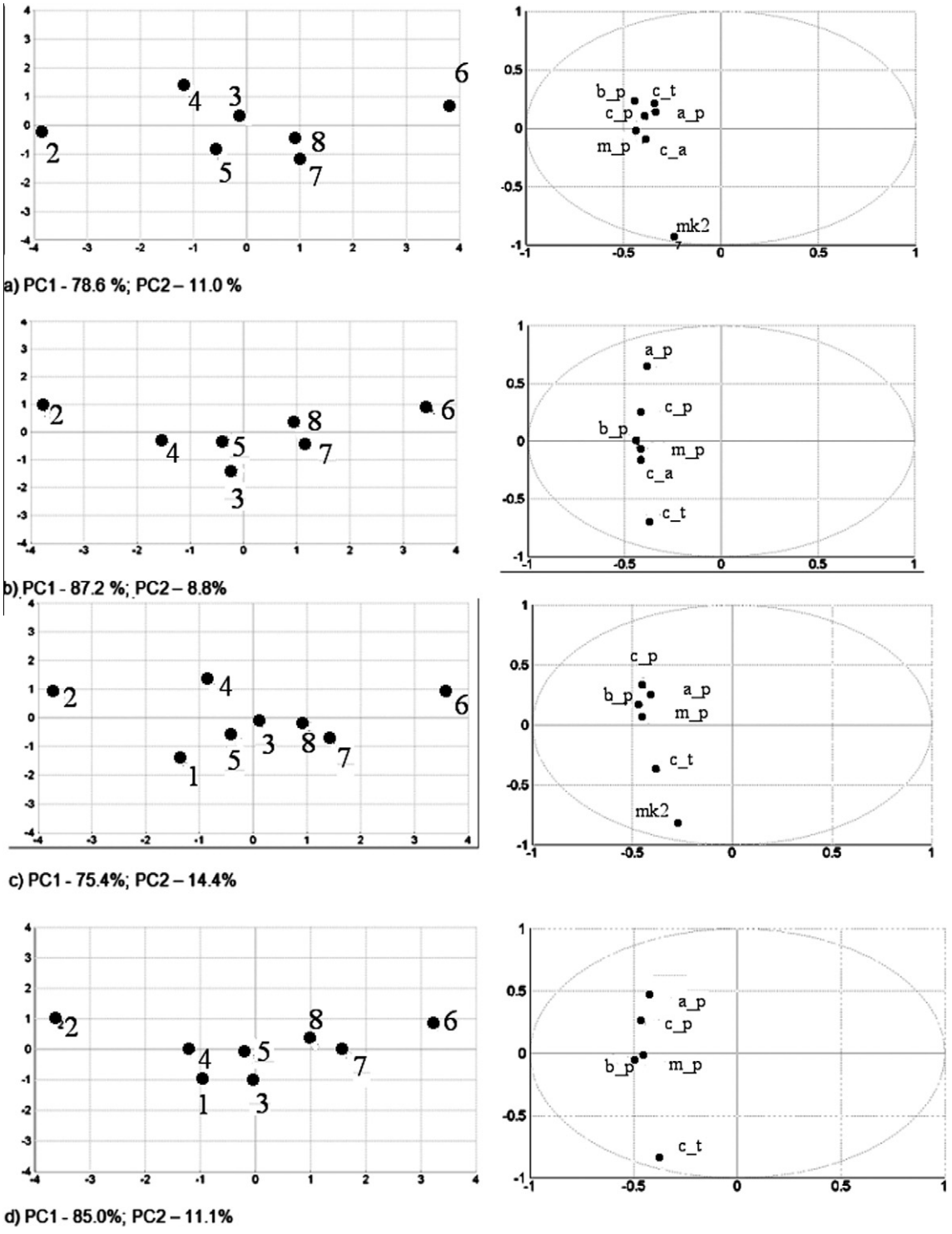

Figure 3. Scores plot (left side) and respective loadings (right side) and values of explained variance by principal components: (a) for all activities excluding azelnidipine (**1**); (b) for anti-parasitic activities excluding azelnidipine (**1**); (c) for all compounds without *L. (L.) chagasi* amastigotes; (d) for anti-parasitic activity for all compounds without *L. (L.) chagasi* amastigotes. Biological activity labels: c_p = *L. (L.) chagasi* promastigotes; c_a = *L. (L.) chagasi* amastigotes, a_p = *L. (L.) amazonensis* promastigotes, m_p = *L. (L.) major* promastigotes, b_p = *L. (V.) braziliensis* promastigotes, c_t = *T. cruzi* trypomastigotes, mk2 = LLC-MK2 cytotoxicity.

at the same level were mutually incomparable due to the contradictory attributes of anti-protozoan activity and cytotoxicity against mammalian cells.

Based on the PCA plots (Fig. 3a), the compounds could be visualized according to their activities. We demonstrated that all activities contributed negatively to the first principal component, which explained 78.6% of all variance, with compound **2** situated to the left of the horizontal axis, corroborating the Hasse diagram. The second Hasse diagram (Figure 2b—for anti-parasitic activities) excluding azelnidipine generated the following chains: **2** ⩾ **4** ⩾ **7**, **2** ⩾ **4** ⩾ **5** ⩾ **8** ⩾ **6**, and **3** ⩾ **6**, which were very similar to the previously obtained Hasse diagram. Considering the potential anti-parasitic activity, it should be noted that compound 4 was the least cytotoxic against LLC-MK2 cells. The same result was obtained in the PCA plots in Figure 3b, where the first two principal components explained 87.2% and 8.8% of the total variance, respectively.

The next Hasse diagram (Fig. 2c) was generated by comparing all compounds according to their activity, excluding *L. (L.) chagasi* amastigotes activity. We obtained more chains comparing the 1,4-dihydropyridines according to their activities: **1** ⩾ **3** ⩾ **6**, **1** ⩾ **5** ⩾ **8** ⩾ **6**, **2** ⩾ **4** ⩾ **6**, **2** ⩾ **5** ⩾ **7**, and **2** ⩾ **5** ⩾ **8** ⩾ **6**. The PCA plots in Figure 3c corroborated the Hasse diagram; the first two principal components explained 89.8% of the total variance. Considering all of the tested 1,4-dihydropyridines and their anti-protozoan activities in the last diagram (Fig. 2d), the potential activities of compounds **1**, **2**, **3**, 4, and **5** should be highlighted. By comparing these molecules, the obtained chains were: **2** ⩾ **4** ⩾ **5** ⩾ **7**, **2** ⩾ **4** ⩾ **5** ⩾ **8** ⩾ **6**, **1** ⩾ **5** ⩾ **8** ⩾ **6**, **1** ⩾ **5** ⩾ **7**, **3** ⩾ **7**, and finally **3** ⩾ **6**. Based on PCA plots (Fig. 3d), we confirmed the high activities of azelnidipine (**1**), amlodipine (**2**), and lercanidipine (**4**).

Based on the structures of the tested compounds, they were separated into sets for comparison according to biological activity, which resulted in seven equations with only one or two descriptors (Table 3). Only 13 different descriptors were selected and belonged to HATS (autocorrelation descriptors); the H, R, and maximal R indices were suitable for structure–property correlations, although they can also be used as molecular profiles for similarity/diversity analysis studies. Based on spatial autocorrelation, these descriptors encode information of structural fragments and therefore seem to be particularly suitable for describing differences in congeneric series of molecules.[22,23]

In equation 1, generated using the pIC_{50} values against *L. (L.) chagasi* promastigotes, the H6m (positive contribution) was an H index autocorrelation of lag 6 weighted by atomic mass, and all H values provided information on the interaction degree between atom pairs. Lercanidipine (**4**), azelnidipine (**1**), and amlodipine (**2**) presented higher values of this descriptor. Lercanidipine (**4**) and azelnidipine (**1**) contained diphenylpropyl and diphenylmethylazetidin groups, respectively, at position 4 of the 1,4-dihydropyridine ring. R4m was generated by multiplication of the leverage between two atoms and the value of their respective atomic masses, with a topological distance equal to 4, divided by the geometrical distance between them. As a consequence of the superior influence of the two atoms in the molecular form, their atomic masses and the shorter distance between them, a higher value of R4m was found. We also observed that amlodipine (**2**) presented the lowest value of R4m and was the only compound with the 2-aminoethoxy-methyl at position 2 of the pyridine.

Equation 2 was generated using pIC_{50} values against intracellular amastigotes of *L. (L.) chagasi*. HATS6u (negative contribution) was a leverage-unweighted autocorrelation of lag 6 and, as HATS descriptors, it encoded the 3D molecular geometry using the leverage values as atomic weightings. In addition, amlodipine (**2**), lercanidipine (**4**), and nimodipine (7) showed lower HATS6u values. Nifedipine (**6**), which was the least active and smallest molecule, presented the highest value of this descriptor and was the only one with a nitro group in the ortho position.

Equation 3 was generated using pIC_{50} values against *L. (L.) amazonensis* promastigotes. This equation showed H0m (positive contribution); it provided information of autocorrelation over the single atoms using the values of atomic masses. HATS4e (negative contribution) was a leverage-electronegativity weighted autocorrelation of lag 4 and was correlated with HATS6u ($r = 0.87$; see

Table 3
Multiple linear regression equations and statistical parameters generated using GETAWAY descriptors and genetic algorithm of variable selection

Activity	Equation
L. (L.) chagasi promastigotes	pEC_{50} = 3.38(±1.31) **H6m** − 6.34(±2.30) **R4m** + 7.23(±1.26) (**I**) (n = 8; r^2 = 0.94; s = 0.15; F = 39.1; Q^2_{cv} = 0.81; S_{PRESS} = 0.22)
L. (L.) chagasi amastigotes	pEC_{50} = −4.74(±1.95) **HATS6u** + 6.21(±0.68) (**II**) (n = 7; r^2 = 0.89; s = 0.18; F = 39.3; Q^2_{cv} = 0.80; S_{PRESS} = 0.19)
L. (L.) amazonensis promastigotes	pEC_{50} = 2.31(±1.92) **H0m** − 11.78(±5.69) **HATS4e** + 3.77(±3.06) (**III**) (n = 8; r^2 = 0.86; s = 0.25; F = 15.4; Q^2_{cv} = 0.73; S_{PRESS} = 0.27)
L. (L.) major promastigotes	pEC_{50} = 2.08(±1.76) **H0m** − 27.06(±12.73) **HATS4m** + 3.47 (±2.64) (**IV**) (n = 8; r^2 = 0.86; s = 0.22; F = 15.3; Q^2_{cv} = 0.72; S_{PRESS} = 0.24)
L. (V.) braziliensis promastigotes	pEC_{50} = −2.86(±0.86) **HATS8u** + 33.16(±8.92) **R6m⁺** + 5.59(±0.42) (**V**) (n = 8; r^2 = 0.95; s = 0.12; F = 44.8; Q^2_{cv} = 0.82; S_{PRESS} = 0.18)
T. cruzi trypomastigotes	pEC_{50} = −116.76(±55.24) **R8u⁺** + 12.08 (±2.37) (**VI**) (n = 8; r^2 = 0.82; s = 0.23; F = 26.8; Q^2_{cv} = 0.74; S_{PRESS} = 0.23)
LLC-MK2 cytotoxicity	pEC_{50} = 14.90(±6.30) **HATS3u** + 1.66 (±0.65) **H2e** − 5.50(±3.13) (**VII**) (n = 8; r^2 = 0.92; s = 0.14; F = 30.3; Q^2_{cv} = 0.86; S_{PRESS} = 0.15)

Table 4
Correlation matrix for GETAWAY descriptors selected with equations 1–7

	HATS3u	HATS6u	HATS8u	H0m	H6m	HATS4m	HATS4e	H2e	R8u+	R4m	R6m+
HATS3u	**1.00**	−0.02	0.35	0.66	−0.52	0.19	0.32	−0.64	0.06	−0.58	0.56
HATS6u		**1.00**	**0.73**	0.58	−0.45	**0.87**	**0.84**	**−0.92**	**0.87**	0.35	−0.04
HATS8u			**1.00**	0.63	−0.48	0.65	0.68	**−0.89**	**0.92**	−0.14	0.46
H0m				**1.00**	−0.18	0.81	0.77	**−0.76**	0.59	0.40	0.45
H6m					**1.00**	−0.51	−0.72	0.70	−0.37	0.20	0.02
HATS4m						**1.00**	0.96	**−0.88**	0.69	0.46	−0.18
HATS4e							**1.00**	**−0.76**	**0.71**	**0.70**	−0.63
H2e								**1.00**	**−0.90**	0.22	−0.63
R8u+									**1.00**	0.01	0.32
R4m										**1.00**	**−0.80**
R6m+											**1.00**

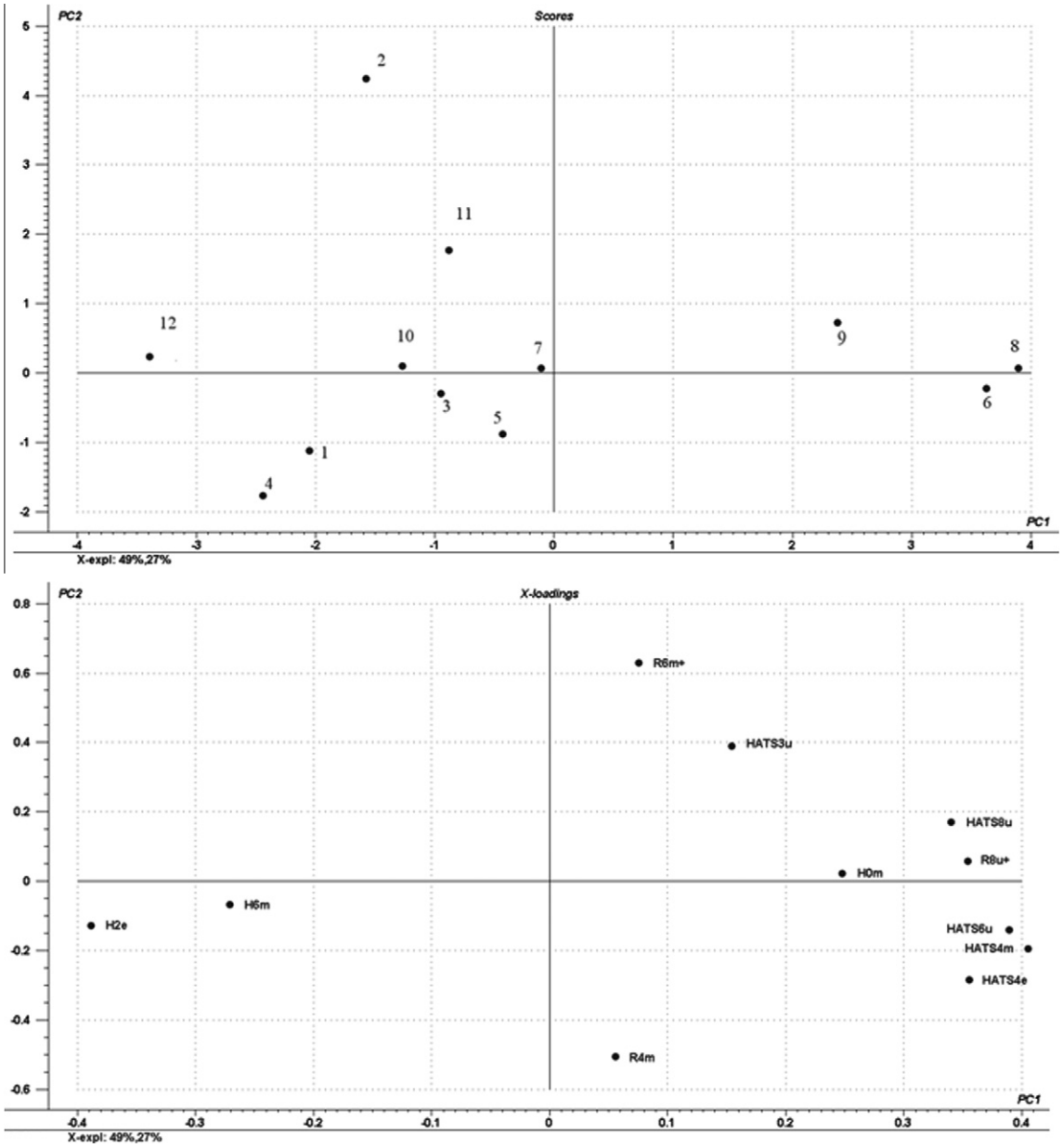

Figure 4. Scores plot (left side) and respective loadings (right side) and values of explained variance by principal components for the compound training set (compounds **1**–**8**), isradipine and lacidipine (compounds **9** and **10**) and new designed 1,4-dihydropyridine analogues (compounds **11** and **12**) using the selected GETAWAY descriptors with equations 1–7.

Table 4). Amlodipine (**2**), which was the most active molecule among the tested 1,4-dihydropyridynes, showed the lowest value of HATS4m, while nifedipine (**6**) and nitrendipine (**8**) presented the highest values.

Equation 4 was generated using pIC_{50} values against *L. (L.) major* promastigotes. This equation showed H0m (positive contribution) and was discussed in equation 3. It was an H index autocorrelation of lag 0 weighted by atomic mass. As explained before, it provided information on autocorrelation over the single atoms. Nifedipine (**6**) showed the smallest value of H0m, was the least active compound and was the only one with a nitro group on the benzene ring at the ortho position. HATS4m (negative contribution) was a leverage-autocorrelation of lag 4 weighted by the atomic masses and was highly correlated ($r = 0.96$—Table 4) with HATS4e. Nifedipine (**6**) and nitrendipine (**8**) showed the largest values of HATS4m. Amlodipine (**2**), the most active compound, showed the smallest value of this descriptor. This higher value of $R6m^+$ for amlodipine was overstated due to the chlorine atom, which had a topological distance of 6 relative to the carboxyl oxygen.

Equation 5 was obtained using pIC_{50} values against *L. (V.) braziliensis* promastigotes. HATS8u (negative contribution) was a leverage-unweighted autocorrelation of lag 8 and was correlated with H2e ($r = -0.89$; see Table 4). Nifedipine (**6**) and nitrendipine (**8**) showed the largest values of this descriptor, and amlodipine (**2**) presented a value of R6m+ (positive contribution). This higher value of $R6m^+$ for amlodipine was overstated due to the chlorine atom, which had a topological distance of 6 relative to the carboxyl oxygen.

$R8u^+$ (negative contribution) was the only selected descriptor from equation 6, which was generated using pIC_{50} values against *T. cruzi* trypomastigotes and was the maximal contribution to the autocorrelation at lag 8 that was unweighted with respect to the influence/distance matrix R. This descriptor was highly correlated with HATS8u ($r = 0.92$). Azelnidipine (**1**) showed lower values of

this descriptor and nifedipine (**6**) showed the largest value, as observed in equation 3.

The model generated from the cytotoxicity pIC_{50} values against LLC-MK2 cells showed only positive contributions of descriptors HATS3u, H2e. HATS3u was uncorrelated with all other descriptors selected by the seven generated equations (r <0.7—Table 4). Lercanidipine (**4**), which was the least cytotoxic compound, presented the smallest value of HATS3u. Amlodipine (**2**), azelnidipine (**1**), nicardipine (**5**), and nimodipine (**7**) showed higher values of HATS3u and H2e. H2e was an electronic descriptor, but was highly correlated with others steric indexes as HATS6u, HATS8u, and HATS4m (r >0.88; Table 4).

The variables selected in all equations were used to perform a PCA to analyze the distributions in two dimensions and verify relationships according to the physicochemical features encoded by selected descriptors and their activities. In this step, two other 1,4-dihydropyridines, isradipine (3-*O*-methyl-5-*O*-propan-2-yl-4-(2,1,3-benzoxadiazol-4-yl)-2,6-dimethyl-1,4-dihydropyridine-3,5-dicarboxylate) and lacidipine (diethyl-2,6-dimethyl-4-[2-[(*E*)-3-[(2-methylpropan-2-yl)oxy]-3-oxoprop-1-enyl]phenyl]-1,4-dihydropyridine-3,5-dicarboxylate), were selected from the literature. In vivo activity of lacidipine (**10**) against *L. (L.) donovani*[7] and in vitro activity of isradipine (**9**) against *T. cruzi* epimastigotes[19] has been reported.

The first two principal components, generated using the 11 descriptors selected by the seven equations, explained 76% of the total variance (PC1—49% and PC2—27%). Analyzing both plots, scores and loadings, it was possible to visualize the similarity among the compounds and their activities. Azelnidipine (**1**) and lercanidipine (**4**) were positioned close to the left side on the horizontal axis (first component). Both compounds showed almost the same similarity when comparing the Hasse diagrams in Figure 2 and the PCA scores plots in Figure 3. Regarding their activities, the substantial differences between these molecules was that azelnidipine (**1**) was the most cytotoxic against mammalian cells and the most active against *T. cruzi*. The scores plot in Figure 4 could not differentiate between the compounds when one considered their cytotoxicity, but it was clear that the first component discriminated the 1,4-dihydropyridines with respect to their anti-leishmanial activity.

Cilnidipine (**3**) and nicardipine (**5**) presented the same behavior, but it is important to highlight that cilnidipine (**3**) demonstrated a higher anti-trypanosomal activity but lower cytotoxicity than nicardipine (**5**). Thus, amlodipine (**2**) was the most active against *Leishmania* and azelnidipine (**1**) was the most cytotoxic compound. Both compounds could be considered more active than nimodipine (**7**), which was positioned next to the center of the plot. Nifedipine (**6**) and nitrendipine (**8**) were located in the second and first quadrants, which could be considered to contain less active compounds.

Amlodipine (**2**) was positioned on the left-up side of the third quadrant, away from the active and inactive compounds. Therefore, amlodipine was an outlier, probably because this was the only compound with chloride atom on the phenyl group at the para position and a 2-aminoethoxymethyl at position 6 of the dihydropyridine fragment. In our analysis, isradipine (**9**) was located in the first quadrant close to the inactive compounds nifedipine (**6**) and nitrendipine (**8**) against *Leishmania.* Lacidipine (**10**) was close to nimodipine (**7**), a more active compound than nifedipine (**6**); consequently, this compound might be more active than isradipine (**9**).

We designed two new 1,4-dihydropyridines analogues (Fig. 5) using the analysis obtained by QSAR equation and PCA with the selected descriptors. The compounds (*S*)-3-ethyl 5-methyl 2-((2-aminoethoxy)methyl)-1,4-dihydro-4-(3-nitrophenyl)pyridine-3,5-dicarboxylate (**11**) and (*S*)-3-[2,2-dimethyl-3-(methyl-phenyl-amino)-propyl]-5-methyl-2-(2-amino-ethoxymethyl)-4-(3-nitro-phenyl)-1,4-dihydro-pyridine-3,5-dicarboxylate (**12**) were inserted in PCA analysis (Fig. 4) and were located in the second quadrant. The compound **12** was in an opposite position of nifedipine (**6**) and nitrendipine (**8**), which were inactive molecules on the first component. The pIC_{50} anti-protozoan values generated using equations 1–6 were promising for both compounds and were shown in Table 5. The cytotoxicity against LLC-MK2 cells was generated using equation 7 and was listed in the same table.

The Hasse diagrams and the PCAs generated using the anti-protozoan and cytotoxicity values of the seven different bioassays supported the comparison and classification of these compounds, and allowed grouping of the 1,4-dihydropyridines. The selected GETAWAY descriptors using the multiple linear regressions and genetic algorithm were able to differentiate the most active compounds. The equations and PCA helped to discriminate some physicochemical (mainly steric) characteristics that were related to structural features that influenced activity. Regarding these characteristics, the diphenylpropyl group at position 4 of the 1,4-dihydropyridine and chloride atom at the ortho position of phenyl group were important; but it was also clear that these features resulted in increased cytotoxicity.

The methodology used in this study could be used as a tool for the development of new potential anti-protozoan agents based on 1,4-dihydropyridines, or even as filters for virtual screenings. However, pharmacokinetic studies using calculated molecular properties from 3D molecular fields of interaction energies is an essential strategy to the rational modification of physicochemical properties to achieve a desired ADME (absorption, distribution, metabolism, and excretion) profile. Furthermore, computational approaches for the correlation of molecular structures with

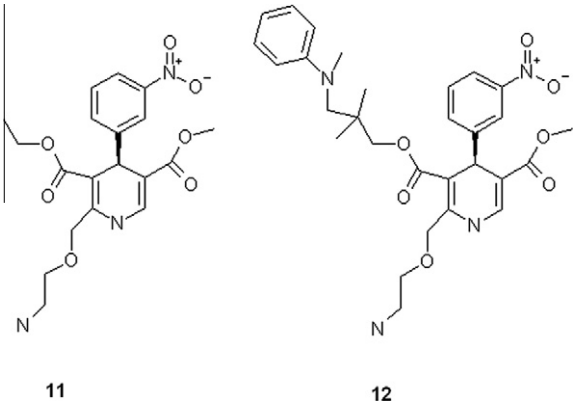

Figure 5. Chemical structures of designed analogues of 1,4-dihydropyridines. Compound **11**: 3-ethyl 5-methyl 2-((2-aminoethoxy)methyl)-1,4-dihydro-4-(3-nitrophenyl)pyridine-3,5-dicarboxylate; **12**: 3-[2,2-dimethyl-3-(methyl-phenyl-amino)-propyl]-5-methyl-2-((2-aminoethoxy)methyl)-4-(3-nitro-phenyl)-1,4-dihydro-pyridine-3,5-dicarboxylate.

Table 5
pIC_{50} and IC_{50} (μM) predicted values by multiple linear equations 1–7 of new designed 1,4-dihydropyridines analogues (compounds **11** and **12**)

Activity	pIC_{50} values		IC_{50} values (μM)	
	Compound **11**	Compound **12**	Compound **11**	Compound **12**
L. (L.) chagasi promastigotes	4.83	5.35	14.79	4.47
L. (L.) chagasi amastigotes	5.11	5.19	7.76	6.46
L. (L.) amazonensis promastigotes	5.08	4.97	8.32	10.72
L. (L.) major promastigotes	5.05	5.21	8.91	6.17
L. (V.) braziliensis promastigotes	4.61	5.22	24.55	6.03
T. cruzi trypomastigotes	4.82	5.52	15.14	3.02
LLC-MK2 cytotoxicity	4.35	4.20	44.67	63.10

pharmacokinetic properties using the Volsurf[24] could also be a suitable strategy for detailed analysis.

3. Conclusion

The 1,4-dihydropyridines showed promising activity against *Leishmania* and *Trypanosoma* parasites. The QSAR provided useful information about the structural features required for the anti-protozoan activity, including the diphenylpropyl and diphenylmethylazetidin groups at position 4 of the 1,4-dihydropyridine ring. The position 2 of the 1,4-dihydropyridine ring was determinant for IC_{50} values. The predicted molecules could be used as new leads for the development of more selective compounds. The 1,4-dihydropyridines represent an important class of compounds, and further investigations into their mode of action could be useful in the development of new agents against Leishmaniasis and Chagas' disease.

4. Experimental

4.1. Materials

Lipopolysaccharide (LPS), sodium dodecyl sulfate (SDS), 3-[4,5-dimethylthiazol-2-yl]-2,5-diphenyltetrazolium bromide (Thiazol blue; MTT), M-199, RPMI-PR$^-$ 1640 medium (without phenol red), azelnidipine (3-*O*-(1-benzhydrylazetidin-3-yl) 5-*O*-propan-2-yl 2-amino-6-methyl-4-(3-nitrophenyl)-1,4-dihydropyridine-3,5-dicarboxylate), amlodipine (3-*O*-ethyl 5-*O*-methyl 2-(2-aminoethoxymethyl)-4-(2-chlorophenyl)-6-methyl-1,4-dihydropyridine-3,5-dicarboxylate), cilnidipine (3-*O*-(2-methoxyethyl) 5-*O*-[(*E*)-3-phenylprop-2-enyl] 2,6-dimethyl-4-(3-nitrophenyl)-1,4-dihydropyridine-3,5-dicarboxylate), lercanidipine (3-*O*-[1-[3,3-diphenylpropyl(methyl)amino]-2-methylpropan-2-yl] 5-*O*-methyl 2,6-dimethyl-4-(3-nitrophenyl)-1,4-dihydropyridine-3,5-dicarboxylate), nicardipine (3-*O*-[2-[benzyl(methyl)amino]ethyl] 5-*O*-methyl 2,6-dimethyl-4-(3-nitrophenyl)-1,4-dihydropyridine-3,5-dicarboxylate), nifedipine (chemical name dimethyl 2,6-dimethyl-4-(2-nitrophenyl)-1,4-dihydropyridine-3,5-dicarboxylate), nimodipine (5-*O*-(2-methoxyethyl) 3-*O*-propan-2-yl 2,6-dimethyl-4-(3-nitrophenyl)-1,4-dihydropyridine-3,5-dicarboxylate) and nitrendipine (3-*O*-ethyl 5-*O*-methyl 2,6-dimethyl-4-(3-nitrophenyl)-1,4-dihydropyridine-3,5-dicarboxylate) were purchased from Sigma–Aldrich. Pentavalent antimony (Glucantime®) was obtained from Aventis-Pharma-Brazil, pentamidine was from Sideron (Brazil) and other analytical reagents were purchased from Sigma (St. Louis, MO, USA).

4.2. Bioassays procedures

BALB/c mice and Golden hamsters were supplied by the animal breeding facility at the Instituto Adolfo Lutz of São Paulo and maintained in sterilized cages under a controlled environment, receiving water and food *ad libitum*. Animal procedures were performed with the approval of the Research Ethics Commission and in agreement with the Guide for the Care and Use of Laboratory Animals from the National Academy of Sciences (http://www.nas.edu).

4.3. Parasite maintenance

Isolated promastigotes of *L. (L.) amazonensis* (WHO/BR/00/LT0016), *L. (V.) braziliensis* (MHO/BR/75/M2903), *L. (L.) chagasi* (MHOM/BR/1972/LD) and *L. (L.) major* (MHOM/1L/80/Fredlin) were maintained in M-199 medium supplemented with 10% calf serum and 0.25% hemin at 24 °C. *L. (L.) chagasi* was maintained in Golden hamsters up to approximately 60–70 days post-infection. *L. (L.) chagasi* amastigotes were obtained from the spleen by differential centrifugation at 60–70th day post-infection. *T. cruzi* trypomastigotes (Y strain) were maintained in LLC-MK2 (ATCC CCL 7) cells using RPMI-1640 medium supplemented with 2% calf serum at 37 °C.

4.4. Determination of the anti-leishmanial activity

To determine the 50% inhibitory concentration (IC_{50} value) against *Leishmania* promastigotes, drugs were dissolved previously in dimethyl sulphoxide (DMSO) and diluted with M-199 medium in 96-well microplates to the highest concentration of 100 μg/m*L*. Each drug was tested twice at eight concentrations prepared at twofold dilution steps. Promastigotes were counted in a Neubauer hemocytometer and seeded at 1×10^6/well with a final volume of 150 μ*L*. Controls with DMSO and without drugs were performed. Pentamidine was used as a standard drug. The plate was incubated for 24 h at 24 °C and the viability of promastigotes was verified by morphology in the light microscopy and the diphenyltetrazolium assay—MTT.[26] Briefly, MTT (5 mg/mL) was dissolved in PBS, sterilized through 0.22 mm membranes and added, 20 μL/well, for 4 h at 24 °C. Promastigotes were incubated without compounds and used as viability contro*L*. Formazan extraction was performed using 10% SDS for 18 h (80 μL/well) at 24 °C and the optical density (OD) was determined in a Multiskan MS (UNISCIENCE) at 550 nm. The data analysis was done in Graph Pad Prism 5.0 software. 100% viability was expressed based on the OD of control promastigotes, after normalization. Those extracts presenting anti-leishmanial activity were tested against intracellular amastigotes of *L. (L.) chagasi*. Briefly, peritoneal macrophages were obtained as described previously and seeded for 24 h at 4×10^5/well in 24-wells plates before infection with *L. (L.) chagasi* amastigotes, which was made at a ratio 1:10 (macrophage/amastigotes) for 18 h at 37 °C in a 5% CO_2 humidified incubator. Infected macrophages were incubated at 37 °C with the test drugs for 120 h at the same conditions described above. Macrophages incubated without drugs were used for control (100% infected). Glucantime was used as a standard drug. At the end of the assay macrophages were fixed with methanol and stained with Giemsa. The parasite burden was determined by the number of infected macrophages (out of 400 cells in duplicate). The data were analyzed using Graph Pad Prism 5.0, which considered the mean of two performed assays in duplicate.

4.5. Determination of the anti-trypanosomal activity

In order to determine the anti-trypanosomal effect of the test drugs against culture trypomastigotes of *T. cruzi*, the drugs were dissolved in DMSO and diluted in RPMI-1640 medium to determine the 50% inhibitory concentration (IC_{50} value) as described above for the anti-leishmanial assay. Free trypomastigotes obtained from LLC-MK2 cultures were counted in a Neubauer hemocytometer and seeded at 1×10^6/well in 96-well microplates. Test drugs were incubated to the highest concentration of 100 μg/mL for 48 h at 37 °C in a 5% CO_2 humidified incubator. Benznidazole was used as standard drug at different concentrations (twofold dilutions). The viability of the trypomastigotes was based in the cellular conversion of the soluble tetrazolium salt MTT (20 μL/well) into the insoluble formazan by mitochondrial enzymes. The formazan extraction was carried out with 10% SDS for 18 h (80 μL/well) at 24 °C as described previously. The number of living trypomastigotes was determined indirectly by the OD at 550 nm. The data analysis was performed using Graph Pad Prism 5.0 software, which considered the mean of two performed assays in duplicate.

4.6. Determination of the cytotoxicity against mammalian cells

Kidney *Rhesus* monkey cells (LLC-MK2) were seeded at 4×10^4 cells/well in 96-well microplates and incubated with drugs to the highest concentration of 200 μg/mL for 48 h at 37 °C in a 5% CO_2 humidified incubator. The viability of cells was determined by the MTT assay as described above and was confirmed by comparing the morphology of the control group via light microscopy. Glucantime, pentamidine, and benznidazole were used as standard drugs. Control cells were incubated in the presence of DMSO and without drugs. The sigmoid dose–response analysis was made using Graph Pad Prism 5.0 software, which considered the mean of two performed assays in duplicate.

4.7. Determination of the hemolytic activity

The capacity of the tested drugs to induce hemolysis at concentrations close to the IC_{50} against *Leishmania* was verified using erythrocytes.[25] BALB/c mice erythrocytes were collected in 0.15 M citrate buffer, pH 7.4, and washed by centrifugation with 0.15 M phosphate-buffered saline, pH 7.4. To determine the hemolytic activity, the drugs were incubated for 3 h at 25 °C with a 3% suspension of erythrocytes in 96-well U-shape microplates. Hemolysis was determined by reading the supernatant absorbance with a plate spectrophotometer (Labsystems; Multiskan EX) at 550 nm. A suspension of erythrocytes incubated with water was used as a positive control (100% hemolysis).

4.8. Statistical analysis

Data represent the mean and standard deviation of duplicate samples from two or three independent assays. The IC_{50} values were calculated using sigmoidal dose–response curves in Graph Pad Prism 5.0 software and the standard error are indicated. In order to compare the activities among the 1,4-dihydropyridines, Principal Component Analysis (PCA) and Hasse diagrams were used.

4.9. Molecular modeling

Molecular modeling computations were performed on SPARTAN for Windows v. 4.0 software (Wavefunction, Inc., Irvine, CA). The compounds (Figs. 1 and 5) were subjected to geometrical optimization and conformational analysis (systematic analysis with dihedral angle rotated at each 30°). The AM1 semi-empirical quantum chemical method was used (Austin Model 1)[27] and the root mean square (RMS) gradient value of 0.001 kcal/mol was the termination condition. Energy minimized molecules were saved as MDL MolFiles for computing various molecular descriptors using DRAGON Professional Version 5.4.[28]

4.10. Molecular descriptors

The DRAGON program generated different groups of descriptors: 2D autocorrelations,[29–31] geometrical descriptors,[32–34] RDF descriptors,[35] 3D-MoRSE descriptors[36,37] and Weighted Holistic Invariant Molecular (WHIM)[38] and GETAWAY descriptors (Geometry Topology, and Atom-Weights Assembly),[22,23] among others.

4.11. Variable selection

Constant variables were excluded, as well as those that presented only a different value of the series (near constant variable). For the remaining descriptors, pair wise correlation (r <0.99) analysis was performed to exclude those that were highly correlated.[39] Thus, the number of GETAWAY descriptors used in our calculations was reduced to 89 descriptors.

The MobyDigs program was used for the calculation of regression models, which were based on pIC_{50} ($-\log IC_{50}$) values using genetic algorithms.[40] The search for the best models (highest value of coefficient of internal prediction Q^2_{cv}—leave one out) was performed using ordinary least squares regression (OLS) under the Genetic Algorithm (GA) approach, that is, by the Variable Subset Selection-Genetic Algorithm (VSSGA) method. In the GA terminology, a population was characterized by a set of candidate variables (the genetic heritage of the population) and was constituted by individuals and models made of one or more population variables.[41]

Acknowledgments

This work was supported by Fundação de Amparo à Pesquisa do Estado de São Paulo (FAPESP 08/09260-7). We also acknowledge the CNPq scientific research award given to A.G.T. and the FAPESP scholarship given to J.Q.R. (08/11434-3).

References and notes

1. Abernethy, D. R.; Schwartz, J. B. *N. Eng. J. Med.* **1999**, *341*, 1447. Additional information: PubChem. http://www.ncbi.nlm.nih.gov/sites/entrez?cmd=search&db=mesh&term=Calcium%20Channel%20Blockers[mh. 2009].
2. Bitonti, A. J.; Sjoersdma, A.; McCann, P. P.; Kyle, D. E.; Oduola, A. M. J.; Rossan, R. N.; Milhous, W. K.; Davidson, D. E. *Science* **1988**, *242*, 1301.
3. Safa, A. R. C.; Glover, J. L.; Sewell, M. B.; Meyers, M. B.; Biedler, J. L.; Felsted, R. L. *J. Biol. Chem.* **1987**, *262*, 7884.
4. Martin, S. K.; Oduola, A. M.; Milhous, W. K. *Science* **1987**, *235*, 899.
5. Neal, R. A.; van Bueren, J.; McCoy, N. G.; Iwobi, M. *Trans. R. Soc. Trop. Med. Hyg.* **1989**, *83*, 197.
6. Valiathan, R.; Dubey, M. L.; Mahajan, R. C.; Malla, N. *Exp. Parasitol.* **2006**, *114*, 103.
7. Palit, P.; Ali, N. *Antimicrob. Agents Chemother.* **2008**, *52*, 374.
8. Tempone, A. G.; Taniwaki, N. N.; Reimão, J. Q. *Parasitol. Res.* **2009**, *105*, 499.
9. Todeschini, R.; Consonni, V. *Handbook of Molecular Descriptors*; Wiley-VCH: Weinheim, Germany, 2000.
10. Kubinyi, H. *QSAR: Hansch analysis and related approaches*; VCH: New York, 1993.
11. Kier, L. B.; Hall, L. H. *J. Chem. Inf. Comput. Sci.* **2000**, *40*, 784.
12. García-Domenech, R.; García, F. J.; Soler, R. M.; Gálvez, J.; Anton-Fos, G. M.; de Julián-Ortiz, J. V. *Quant. Struct.-Act. Relat.* **1996**, *15*, 1.
13. Julián-Ortiz, J. V.; Gálvez, J.; Muñoz-Collado, C.; García-Domenech, R.; Gimeno-Cardona, C. *J. Med. Chem.* **1999**, *42*, 3308.
14. Gregorio Alapont, C.; García-Domenech, R.; Gálvez, J.; Ros, M. J.; Wolski, S.; García, M. D. *Bioorg. Med. Chem. Lett.* **2000**, *10*, 2033.
15. Gozalbes, R.; Brun-Pascaud, M.; García-Domenech, R.; Gálvez, J.; Girard, P. M.; Doucet, J. P.; Derouin, F. *Antimicrob. Agents Chemother.* **2000**, *44*, 2764.
16. Li, X.; Ruan, G. R.; Lu, W. L.; Hong, H. Y.; Liang, G. W.; Zhang, Y. T.; Liu, Y.; Long, C.; Ma, X.; Yuan, L.; Wang, J. C.; Zhang, X.; Zhang, Q. *J. Controlled Release* **2006**, *112*, 186.
17. Taylor, J. M.; Simpson, R. U. *Cancer Res.* **1992**, *52*, 2413.
18. Kumar, K. A.; Ganguly, K.; Mazumdar, K.; Dutta, N. K.; Dastidar, S. G.; Chakrabarty, A. N. *Acta Microbiol. Pol.* **2003**, *52*, 285.
19. Nuñez-Vergara, L. J.; Squella, J. A.; Bollo-Dragnic, S.; Marín-Catalán, R.; Pino, L.; Díaz-Araya, G.; Letelier, M. E. *Gen. Pharmacol.* **1998**, *30*, 85.
20. Tasdemir, D.; Kaiser, M.; Brun, R.; Yardley, V.; Schmidt, T.; Tosun, F.; Ruedi, P. *Antimicrob. Agents Chemother.* **2006**, *50*, 1352.
21. Allen, G. S.; Ahn, H. S.; Preziosi, T. J.; Battye, R.; Boone, S. C.; Boone, S. C.; Chou, S. N.; Kelly, D. L.; Weir, B. K.; Crabbe, R. A.; Lavik, P. J.; Rosenbloom, S. B.; Dorsey, F. C.; Ingram, C. R.; Mellits, D. E.; Bertsch, L. A.; Boisvert, D. P.; Hundley, M. B.; Johnson, R. K.; Strom, J. A.; Transou, C. R. *N. Eng. J. Med.* **1993**, *11*, 619.
22. Consonni, V.; Todeschini, R.; Pavan, M. *J. Chem. Inf. Comput. Sci.* **2002**, *42*, 682.
23. Consonni, V.; Todeschini, R.; Pavan, M.; Gramatica, P. *J. Chem. Inf. Comput. Sci.* **2002**, *42*, 693.
24. Crivori, P.; Cruciani, G.; Carrupt, P. A.; Testa, B. *Med. Chem.* **2000**, *43*, 2204.
25. Conceição, K.; Konno, K.; Richardson, M.; Antoniazzi, M. M.; Jared, C.; Daffre, S.; Camargo, A. C.; Pimenta, D. C. *Peptides* **2006**, *27*, 3092.
26. Tada, H.; Shiho, O.; Kuroshima, K.; Koyama, M.; Tsukamoto, K. *J. Immunol. Methods* **1986**, *93*, 157.
27. Dewar, M. J. S.; Healy, E. F.; Holder, A. J.; Yuan, Y. C. *J. Comput. Chem.* **1990**, *11*, 541.
28. Talete, S. R. L. Mobydigs Academic version. Version 1.1—2009—http://www.talete.mi.it.
29. Moran, P. A. P. *Biometrika* **1950**, 37.
30. Geary, R. C. *The Incorporated Statistician* **1954**, *5*, 115.

31. Moreau, G.; Broto, P. *Nouveau J. de Chim.—New J. Chem.* **1980**, *4*, 359.
32. Diudea, M. V.; Horvath, D.; Graovac, A. *J. Chem. Inf. Comput. Sci.* **1995**, *35*, 129.
33. Balaban, A. T. *J. Chem. Inf. Comput. Sci.* **1997**, *37*, 645.
34. Randic, M.; Kleiner, A. F.; Dealba, L. M. *J. Chem. Inf. Comput. Sci.* **1994**, *34*, 277.
35. Hemmer, M. C.; Steinhauer, V.; Gasteiger, J. *Vibrat. Spectrosc.* **1999**, *19*, 151.
36. Gasteiger, J.; Sadowski, J.; Schuur, J.; Selzer, P.; Steinhauer, L.; Steinhauer, V. *J. Chem. Inf. Comput. Sci.* **1996**, *36*, 1030.
37. Schuur, J. H.; Selzer, P.; Gasteiger, J. *J. Chem. Inf. Comput. Sci.* **1996**, *36*, 334.
38. Todeschini, R.; Gramatica, P. *Quant. Struct.-Act. Relat.* **1997**, *16*, 113.
39. Livingstone, D. *Data Analysis for Chemists*; Oxford Science Publications: New York, 1995.
40. Talete, S. R. L. DRAGON for Windows (Software for Molecular Descriptor Calculations). Version 5.4—2006—http://www.talete.mi.it.
41. Leardi, R.; Boggia, R.; Terrile, M. *J. Chemom.* **1992**, *6*, 267.